Neurotoxicology 70 (2019) 62–71

Contents lists available at ScienceDirect

Neurotoxicology

journal homepage: www.elsevier.com/locate/neuro

Full Length Article

Antiapoptotic effect of taurine against NMDA-induced retinal excitotoxicity in rats

Lidawani Lambuk[a], Igor Iezhitsa[a,b,*], Renu Agarwal[a,d], Nor Salmah Bakar[a], Puneet Agarwal[c], Nafeeza Mohd Ismail[c]

[a] Center for Neuroscience Research (NeuRon), Faculty of Medicine, Universiti Teknologi MARA, Sungai Buloh Campus, Sungai Buloh, Selangor, Malaysia
[b] Volgograd State Medical University, Research Institute of Pharmacology, Volgograd, Russia
[c] International Medical University, IMU Clinical School, Seremban, Malaysia
[d] I-PPerForM, Faculty of Medicine, Universiti Teknologi MARA, Sungai Buloh Campus, Selangor, Malaysia

ARTICLE INFO

Keywords:
Glaucoma
Retina
Retinal ganglion cells (RGCs) apoptosis
NMDA
Excitotoxicity
Brain-derived neurotrophic factor (BDNF)
Taurine
Neuroprotection

ABSTRACT

Objective: *N-methyl-D-aspartate* (NMDA) excitotoxicity has been proposed to mediate apoptosis of retinal ganglion cells (RGCs) in glaucoma. Taurine (TAU) has been shown to have neuroprotective properties, thus we examined anti-apoptotic effect of TAU against retinal damage after NMDA exposure.

Methodology: Sprague-Dawley rats were divided into 5 groups of 33 each. Group 1 was administered intravitreally with PBS and group 2 was similarly injected with NMDA (160 nmol). Groups 3, 4 and 5 were injected with TAU (320 nmol) 24 hours before (pre-treatment), in combination (co-treatment) and 24 hours after (post-treatment) NMDA exposure respectively. Seven days after injection, rats were sacrificed; eyes were enucleated, fixed and processed for morphometric analysis, TUNEL and caspase-3 staining. Optic nerve morphology assessment was done using toluidine blue staining. The estimation of BDNF, pro/anti-apoptotic factors (Bax/Bcl-2) and caspase-3 activity in retina was done using ELISA technique.

Results: Severe degenerative changes were observed in retinae after intravitreal NMDA exposure. The retinal morphology in the TAU pre-treated group appeared more similar to the control retinae and demonstrated a higher number of nuclei than the NMDA group both per 100 μm length (by 1.5-fold, $p < 0.001$) and per 100 μm^2 area (by 1.41-fold, $p < 0.05$) of the GCL. After NMDA exposure, visible axonal swelling was observed in optic nerve sections. In comparison with the changes observed in the NMDA treated group, the TAU treated group showed fewer prominent changes; axonal swelling was less frequent and less marked. Additionally, no marked glial cell changes were observed in the TAU-pretreated group. All TAU treated groups, particularly the pre-treated group, showed a significant decrease in the NMDA-induced optic nerve damage, with a 50% reduction ($p < 0.001$) in the mean grading compared to NMDA group. For the same, there was 25% decrease in co- and post-treatment groups, as compared with the NMDA group. Pre-treatment with TAU abolished apoptotic response to NMDA as indicated by decrease in the number of TUNEL- and caspase-3-positive cells. TAU pre-treatment also increased the Bcl-2 level (by 2.80-fold, $p < 0.001$) and decreased the level of Bax (by 34%, $p < 0.01$), and activity of caspase-3 (by 36%, $p < 0.001$) compared to NMDA group.

In conclusion: our study revealed that pre-treatment with TAU prevents NMDA-induced retinal cell apoptosis more effectively than co- and post-treatment with TAU.

1. Introduction

Glaucoma is a group of diseases that are characterised by the progressive degeneration of retinal ganglion cells (RGCs) and their axons. It is the leading cause of irreversible blindness worldwide, and is the second most common cause of blindness after cataract (Baltmr et al., 2010). According to an estimate, more than 60 million people were affected by this ocular disease in 2013 (Tham et al., 2014). The World Health Organisation (WHO) has estimated that approximately 80 million people will be affected by glaucoma by 2020. Almost 4.5 million cases of blindness caused by glaucoma have been reported worldwide and this number is estimated to increase to 11.2 million by 2020 (Quigley and Broman, 2006; Quigley, 2018).

The pathophysiology of glaucoma is currently poorly understood (Agarwal et al., 2009; Ebneter et al., 2011; Casson et al., 2012). The current medical therapy for glaucoma is limited to lowering of

* Corresponding author.

https://doi.org/10.1016/j.neuro.2018.10.009
Received 6 June 2018; Received in revised form 24 October 2018; Accepted 24 October 2018
Available online 30 October 2018

intraocular pressure (IOP), as this has been established as the primary risk factor for the initiation and progression of RGC loss and optic neuropathy (Goldblum & Mittag, 2002; Mozaffarieh & Flammer, 2007). However, elevated IOP is only one of the several risk factors that lead to RGC apoptosis. Recent evidence indicates that lowering of IOP does not prevent glaucoma progression in all patients and that progression can continue despite the effective lowering of IOP (Agarwal et al., 2009; Mozaffarieh & Flammer, 2013). Glutamate-induced excitotoxicity has been implicated as one of the pathogenic mechanisms in glaucoma (Agarwal et al., 2009). The detrimental effect of glutamate on RGCs has been shown to involve NMDA receptors through exposure of the retina to high glutamate levels. In excitotoxicity, glutamate triggers the rise of intracellular Ca^{2+} levels, followed by the upregulation of neuronal NOS (nNOS), dysfunction of mitochondria, reactive oxygen species (ROS) production, endoplasmic reticulum (ER) stress, and release of lysosomal enzymes (Joo et al., 1999; Naskar et al., 2000; Kuehn et al., 2005; Ebneter et al., 2010; Ebneter et al., 2011). Thus, several studies have investigated potential therapeutic strategies for the protection of RGCs by targeting NMDA signalling (Vasudevan et al., 2011; Jafri et al., 2017; Iezhitsa & Agarwal, 2018). Accordingly, NMDA receptor antagonists have been suggested to inhibit the loss of RGCs in excitotoxicity and to delay the progression of loss of vision in glaucoma. However, none of the therapeutic modalities is currently available to prevent RGCs degeneration (Khatib & Martin, 2017).

Taurine (2-aminoethanesulfonic acid; TAU) is the most abundant free amino acid in the retina and it exhibits potent antioxidant properties (Macaione et al., 1974). TAU is also involved in the maintenance of membrane structural integrity and the regulation of calcium binding and transport. It also serves as a neurotransmitter (Militante & Lombardini, 2002; Leon et al., 2009; Lambert et al., 2015). Previous studies have established that TAU can prevent neuronal excitotoxicity (El, 2008; Wu & Prentice., 2010; Froger et al., 2014). In various experimental models, the depletion of TAU has been shown to affect photoreceptor and retinal degeneration (Hayes et al., 1975; Imaki et al., 1987). From the therapeutic point of view, TAU might have the potential to serve as a neuroprotective agent; however, the mechanisms through which TAU produces an anti-apoptotic effect in the NMDA-mediated ocular pathological condition are not well understood. Therefore, the aim of this study was to investigate the neuroprotective role and anti-apoptotic effect of TAU in NMDA-induced retinal excitotoxicity in rats.

2. Material and Methods

2.1. Animals

Sprague-Dawley rats of both genders that weighed 200-250 g (8-12 weeks) were obtained and maintained in the Laboratory Animal Care Unit of University Teknologi MARA under the standard laboratory conditions of a 12-hour cycle of light and dark at a temperature of 23 ± 1.0 °C, with full access to pellet food and water ad libitum. All experiments and animal handling were carried out in accordance with the ARVO Statement for the Use of Animals in Ophthalmic and Vision Research and local animal ethics requirement from the Universiti Teknologi MARA (UiTM), Malaysia. UiTM Care: 215/6/2017(6/10/2017).

2.2. Study design

To evaluate the neuroprotective effect of TAU on NMDA-induced retinal cell apoptosis, Sprague-dawley rats were randomly divided into five groups of 33 each (n = 66 eyes per group) (Fig. 1). The treatments were given as follows:

Group 1: Negative control (**PBS**);

Group 2: Positive control (**NMDA**)

Group 3: Pre-treatment; TAU 24 hours before NMDA (**24TAU + NMDA**)

Group 4: Co-treatment; co-administration of NMDA and TAU (**NMDA + TAU**)

Group 5: Post-treatment; NMDA 24 hours before TAU (**24NMDA + TAU**)

All solutions were administered through intravitreal injection in both eyes after the rats were anaesthetised using intraperitoneal injection of a ketamine and xylazine (Ilium Troy Laboratories, P.L, Australia) mixture (80 mg/kg and 12 mg/kg, respectively). Solutions of NMDA (160 nmol) and TAU (320 nmol) were prepared in 0.1 M phosphate buffered saline (PBS). The injections were done in a volume of 2 µl using 30-gauge needles mounted on 10-µl Hamilton syringe. The tip of the needle was used to puncture the sclera before inserting the Hamilton syringe through the dorsal limbus of the eye. Subsequently, injections were made slowly over 2 minutes to avoid reflux. Tropicamide 1% eye drops were applied to dilate the pupils 10 minutes before the injection. Enucleation of the eye was performed 1 week after

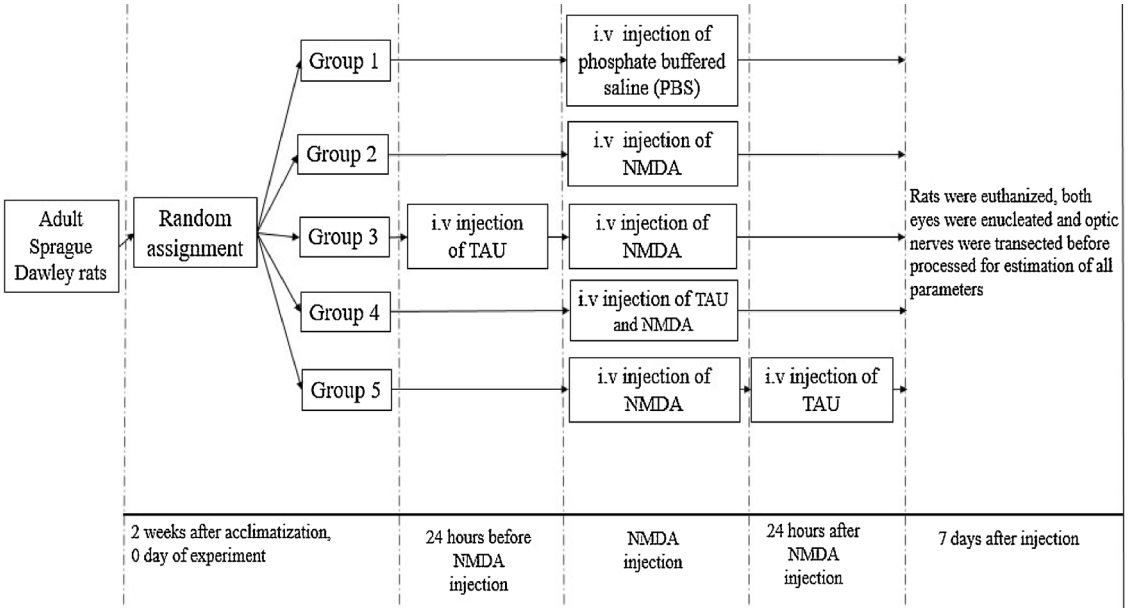

Fig. 1. Experimental design. i.v injection = intravitreal injection.

the injection and the optic nerve was isolated. A suture was applied at 12 O'clock position on the eyeballs for accurate orientation. Both eyes were enucleated for assessment of retinal morphology using haematoxylin and eosin staining (n = 6), the extent of retinal cell apoptosis using terminal deoxynucleotidyl transferase-mediated dUTP nick end-labeling (TUNEL) staining (n = 6) and active caspase-3 (n = 6), retinal brain-derived neurotrophic factor (BDNF) using ELISA (n = 6), retinal anti-apoptotic marker Bcl-2 using ELISA (n = 6), retinal pro-apoptotic marker Bax *(Bcl-2 associated X protein)* using ELISA (n = 6), retinal active caspase-3 assay using ELISA (n = 6). The optic nerves were isolated for optic nerve morphology assessment using toluidine blue staining (n = 6). Tissues for histological and immunohistological examinations were fixed in 10% formaldehyde for 24 hours at room temperature before processing. For all estimation using ELISA, retinae of 2 eyes from the same rat were pooled.

2.3. Retinal morphology assessment

2.3.1. Retinal morphology assessment using haematoxylin and eosin staining

The lenses were removed from the eyeballs which were then bisected at the equator and transferred through a series of graded alcohols for 22 hours before being processed for paraffin embedding. Subsequently, 3-μm-thick sections were cut and stained with haematoxylin and eosin (H&E).

The images of retina were captured using Nikon light microscope connected to a digital camera at a magnification of 20 ×. Retinal morphometric measurements were made using the image analysis software IMAGE J (National Institutes of Health, Bethesda, MA, USA). The number of nuclei per 100 μm length of GCL and the number of nuclei per 100 μm^2 of GCL were estimated. Cells nuclei with a diameter less than 7 μm with distinguishable glial cells and vascular endothelial cells were excluded from the count (Razali et al., 2014; Jafri et al., 2018). The observations were made on retina as a whole that consists of numerous neuronal cells in addition to RGCs. All estimations were made on 3 randomly selected fields of view on each section by 2 independent investigators (Takahata et al., 2003; Ohzeki et al., 2007; Chen et al., 2012; Razali et al., 2014; Lambuk et al., 2016). The average measurement values were used for statistical analysis.

2.4. Optic nerve morphology assessment

2.4.1. Optic nerve morphology assessment through toluidine blue staining

The optic nerve was transacted 1 mm from the eyeball, immersed in 10% formaldehyde overnight and transferred through a series of graded alcohols over 22 hours, before being processed for paraffin embedding. The sections were then taken at 1 μm thickness and stained with 1% Toluidine Blue (Sigma-Aldrich, USA). Six optic nerves per group were obtained from six different animals to establish grade of injury.

The damage to the optic nerve was evaluated by examining full cross-sectional view of optic nerve and analysed by 3 independent observers as described previously (Lambuk et al., 2017; Arfuzir et al., 2017).

The following scale was used to grade the level of injury: (Grade 1) normal axon; (Grade 2) early mild lesions in one area plus moderate axons degeneration; (Grade 3) spread of axon degeneration to another area of the nerve; (Grade 4) progressively greater damage to axons with an equal proportion of normal and degenerated axons; and (Grade 5) degeneration of the majority of axons across all regions of the tissue (Jia et al., 2000).

2.5. Estimation of brain-derived neurotrophic factor (BDNF) in the retina

The level of BDNF in the fresh retinae was measured using commercially available ELISA kits according to the manufacturer's protocol (Elabscience, Wuhan, China). Briefly, retinae were thoroughly cleansed in PBS (pH 7.4) followed by homogenisation in 0.5 ml of radio-Immunoprecipitation assay (RIPA) lysis buffer (150 mM NaCl, 1.0% IGEPAL CA-630, 0.5% sodium deoxycholate, 0.1% SDS, and 50 mM Tris, pH 8.0). To prevent protein degradation, protease inhibitor was added at a ratio of 1 mg retina weight to 10 μl RIPA buffer (Sigma-Aldrich, USA). The tissues were sonicated for 1 minute followed by centrifugation for 13 minutes at 11000 × g at 4 °C to separate the supernatant. One hundred microliters of the samples were pipetted into the appropriate micro ELISA plate wells, which were pre-coated with an antibody that was specific to BDNF, and incubated for 1.5 hours. A temperature of 37 °C was maintained throughout the incubation. A biotinylated detection antibody that was specific for BDNF and Avidin-Horseradish Peroxidase (HRP) conjugate was then added to each well and incubated for 1.5 hours. The free components were then washed away. The substrate solution was added to each well and after the colour turned blue, the enzyme-substrate reaction was discontinued by addition of a sulphuric acid solution. On addition of the sulphuric acid solution, the substrate solution became yellow in colour and the optical density was immediately measured using a microplate reader (Victor X5, Perkin Elmer, US). The estimations were done in duplicate.

2.6. Assessment of apoptosis

2.6.1. Retinal TUNEL assay

A terminal deoxynucleotidyl transferase dUTP nick end labelling (TUNEL) assay was performed to detect the presence of DNA fragmentation in apoptotic cells of the retina, by labelling the terminal end of nucleic acid as described previously (Lambuk et al., 2017; Nor Arfuzir et al., 2018; Arfuzir et al., 2018). The procedure was carried out in accordance with the manufacturer's protocol of the Apo-BrdU-IHCTM *In Situ* DNA Fragmentation Assay Kit (Biovision, USA). Retinal sections of 3 μm-thickness were deparaffinised, followed by antigen retrieval by Proteinase K for 20 minutes and gentle rinsing with PBS for 3 minutes.

The sections were then covered in 100 μl of 3% H_2O_2 (1:10), diluted in methanol, for 5 minutes and rinsed again. The sections were incubated with Br duTP overnight at room temperature (37 °C) and the Br duTP was then washed away by PBS, followed by a 1.5-hour incubation with Anti-Brdu Biotin in a dark humid chamber. A chromogen solution, DAB, was applied to the sections and incubated for 15 minutes before being rinsed 3 times for 2 minutes, followed by methyl green counterstaining for 3 minutes. The slides were then mounted and allowed to air dry followed by observation under a light microscope at a 20× magnification. The images were obtained from 3 randomly selected fields of view from each section. The measurement of apoptotic signal on ganglion cell layer was performed using IMAGE J software (National Institutes of Health, Bethesda, MA, USA) by 2 independent observers. The mean of these measurements was used for further statistical analysis.

2.6.2. Retinal caspase-3 immunohistochemistry

Immunofluorescence staining using an antibody for caspase-3 was performed to detect the presence of an active caspase-3 signal in the GCL. This was conducted as described in previous studies (Arfuzir et al., 2016; Lambuk et al., 2017). The deparaffinised and dehydrated retinal sections were immersed in cold running tap water before the antigen retrieval was performed in 10 mM, 0.05% Tween-20, pH 6.0 of sodium citrate at boiling point for 20 minutes in a domestic microwave. The slides were chilled under cold running tap water for 10 minutes and washed twice with tris buffered saline (TBS) plus 0.025% Triton X-100 for 5 minutes each. The sections were then blocked by peroxidase blocking solution for 30 minutes and washed again with TBS plus 0.025% Triton X-100. This was followed by treatment with 100 μl primary antibody (anti-active + proCaspase 3, ABCAM) diluted with

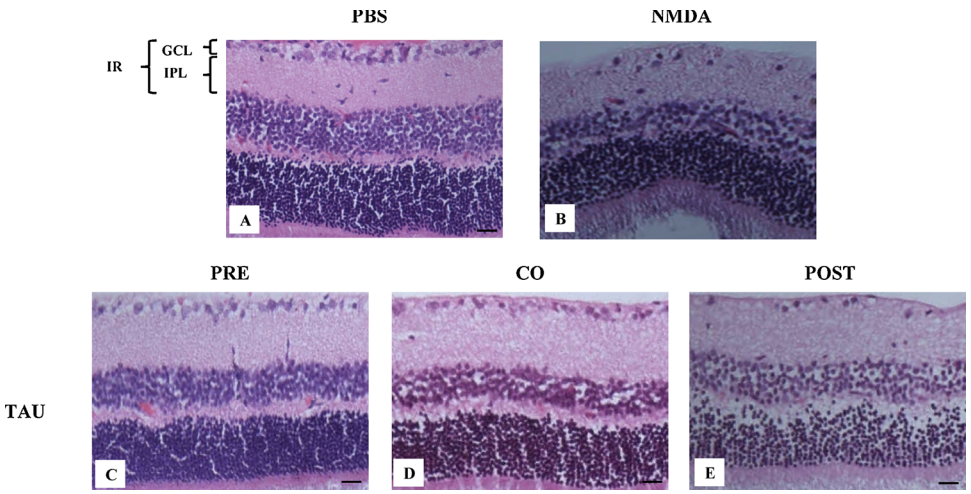

Fig. 2. Representative microphotographs of retinal sections from each of the groups stained with Haematoxylin and Eosin at 20× magnification. Groups **A** (PBS) control, **B** (NMDA), **C** (24TAU + NMDA) pretreatment, **D** (NMDA + TAU) co-treatment, **E** (24NMDA + TAU) post-treatment. GCL= ganglion cell layer, IPL= inner plexiform layer, IR= inner retina. (Scale bar 100 µm).

10 mM Tris 1% BSA (2:98). The slides were incubated overnight at 4 °C. The slides were then rinsed with TBS 0.025% Triton X-100 for 5 minutes to remove the primary antibody completely. The slides were then incubated in secondary antibody conjugated with Texas red fluorochrome (1:1000) (goat anti-rabbit IgG H&L, ABCAM) for 1 hour. After this incubation period, the slides were washed twice with TBS plus 0.025% Triton X-100 for 5 minutes and counter stained with DAPI (1:999), diluted in PBS 1 mM, for 10 minutes before being mounted. Prior to observation, the slides were allowed to air dry completely. The observations were made using an Olympus microscope (BX61TRF-FL-CCD model) in a dark room at excitation 596 nm filter for Texas Red and 358 nm for DAPI (Labes et al., 1999)

2.6.3. Estimation of Bcl-2 and Bax (Bcl-2 associated X protein)

The expression of apoptosis markers, Bcl-2 and Bax, in retinae was estimated using commercially available ELISA kits according to the manufacturer's protocol (Elabscience, Wuhan, China), as described above for the quantification of the retinal BDNF level. All estimations were done in duplicate.

2.6.4. Active caspase-3 assay

Caspase-3 is one of the critical enzymes involved in apoptosis. The caspase-3 colorimetric assay (Sigma-Aldrich, US) was performed based on the hydrolysis of the peptide substrate acetyl-Asp-Glu-Val-Asp p-nitroanilide (Ac-DEVD-pNA) by caspase-3, resulting in the release of the p-nitroaniline (pNA) moiety. The assay was performed according to the manufacturer's protocol. Retinae were washed with PBS (pH 7.4) before recording the wet weight. The retinae were homogenised in 0.3 ml of 1X lysis buffer (50 mM HEPES, pH7.4, 5 nM CHAPS, 5 mM DTT) diluted in 5X with 17 megaohm water. Retinal tissue disruption was carried out by sonication for 1 minute, followed by centrifugation for 20 minutes at 16000 × g at 4 °C and the supernatants were collected. The samples and standards were placed in the appropriate wells, as indicated in the protocol. The reaction was started by adding caspase-3 substrate to each well and gently mixing by shaking. The microplate was incubated at 37 °C for 90 minutes. The concentration of the substrate released was calculated from the absorbance values at 405 nm. All estimations were done in duplicate.

2.6.5. Statistical analysis

All data collected and analysed are presented as the mean ± SD. Statistical comparison was carried out using a one-way ANOVA with Bonferroni's test. $P < 0.05$ was considered significant.

3. Results

3.1. Effect of TAU on the morphology of NMDA-exposed retina (haematoxylin and eosin staining)

Retinal sections stained with H&E were used to evaluate the number of nuclei in the GCL (Fig. 2). Retinal cell nuclei in GCL were more densely packed in the control group than in the NMDA-treated retinae. In comparison, NMDA-exposed retinae showed a lower number of nuclei, by 1.78-fold ($p < 0.001$) per 100 µm length, than the control (PBS group). The retinae in the TAU pre-treated group appeared more similar to the control retinae and demonstrated a higher number of nuclei, by 1.5-fold ($p < 0.001$), than the NMDA group. The nuclear density in TAU co-treatment group was 26% ($p < 0.01$) lower than TAU pre-treatment group and the same in TAU post-treatment group was 27% ($p < 0.001$) lower than TAU pre-treatment group. These groups demonstrated slightly better (not significant) linear cell density compared with the NMDA-treated group, by 1.13- and 1.10- folds, respectively (Fig. 3A).

The number of nuclei per 100 μm^2 area of the GCL in the NMDA-exposed retina was significantly lower than that of the control group by 44% ($p < 0.001$). The number of nuclei was also significantly lower in the TAU co- and post-treated groups than in the control group (PBS), by 25% ($p < 0.05$). TAU pre-treated group demonstrated a higher number of nuclei per 100 μm^2 area of the GCL than the NMDA group, by 1.41-fold ($p < 0.05$). There were no significant differences between the NMDA group and TAU co- and post-treatment groups (Fig. 3B; Table 1).

3.2. Effect of TAU on optic nerve morphology in NMDA-exposed retina (toluidine blue staining)

Fig. 4 represents the morphology of toluidine blue-stained optic nerve cross sections. A normal morphology was observed in the PBS group, with densely arranged uniform axon fibres. Furthermore, glial cell distribution appeared normal in the PBS group. After NMDA exposure, visible axonal swelling was observed. In comparison with the changes observed in the NMDA treated group, the TAU-treated groups showed fewer prominent changes; axonal swelling was less frequent and less marked. No marked glial cell changes were observed in the TAU pre-treated group. The co- and post-treated TAU groups showed more gliosis, a larger vacuolated area and higher degree of nerve fibre degeneration than the TAU pre-treated group.

Quantitative estimations of optic nerve changes showed that the greatest damage occurred in the NMDA group, in comparison with the control and TAU treated groups (Fig. 4F). All TAU treated groups,

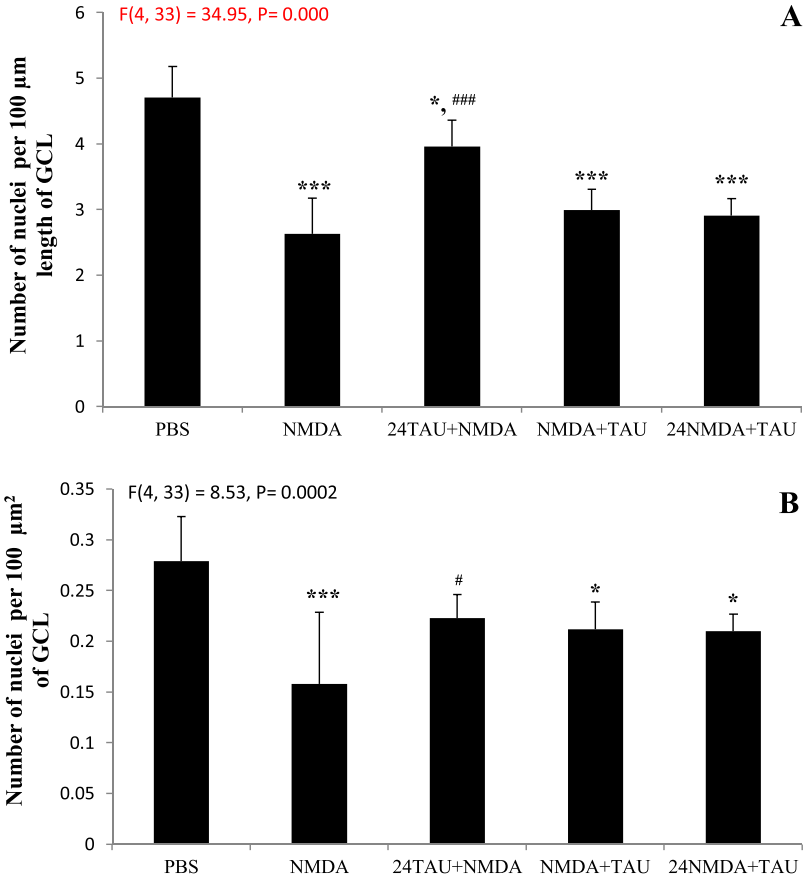

Fig. 3. Graph **A** represents the number of GC nuclei in 100 µm length of GCL. Graph **B** represents the number of GC nuclei in 100 µm^2 of GCL. Groups (PBS) control, (NMDA), (24TAU + NMDA) pretreatment, (NMDA + TAU) co-treatment, (24NMDA + TAU) post-treatment. Data expressed as the mean and SD. Statistical significances were analyzed using one-way ANOVA with Bonferroni correction test: *p < 0.05 versus PBS group, ***p < 0.001 versus PBS group, #p < 0.05 versus NMDA group, ###p < 0.001 versus NMDA group. GCL = ganglion cell layer.

Table 1
Effect of TAU on number of nuclei in GCL after NMDA exposure.

	F-value	PBS	NMDA	24TAU + NMDA	NMDA + TAU	24NMDA + TAU
Number of nuclei per 100 µm^2 of GCL	F(4, 21) = 8.94, P = 0.0002	0.308 ± 0.01	0.158 ± 0.07***	0.344 ± 0.085#	0.304 ± 0.06*	0.279 ± 0.05*
Number of nuclei per 100 µm length of GCL	F(4, 15) = 30.05, P = 0.000	5.837 ± 0.6	2.088 ± 0.46*,###	5.643 ± 1.28***	5.43 ± 0.22***	5.379 ± 0.24***

Notes: Data presented as means ± SD; Groups: **(PBS)** control, **(NMDA)**, **(24TAU + NMDA)** pretreatment, (**NMDA + TAU**) co-treatment, (**24NMDA + TAU**) post-treatment. Statistical significances were analyzed using one-way ANOVA with Bonferroni correction test: *p < 0.05 versus PBS group, ***p < 0.001 versus PBS group, #p < 0.05 versus NMDA group, ###p < 0.001 versus NMDA group. GCL = ganglion cell layer

particularly the pre-treated group, showed a significant decrease in the toxic effect of NMDA, with a 50% decrease ($p < 0.001$) in the mean grading. We also observed a 25% decrease in the mean grading for co- and post-treatment groups as well compared to the NMDA group.

3.3. Effect of TAU on BDNF level in NMDA-exposed retina

In our study, NMDA exposure led to a 72% decrease in the retinal BDNF level ($p < 0.001$) as compared to the PBS group (Fig. 5). The retinal BDNF levels in the TAU pre- and co-treatment groups were higher than that of the NMDA group, with a 3.06- ($p < 0.001$) and 2.47- ($p < 0.05$) fold increase, respectively. However, no significant difference was found between the TAU post-treatment and the NMDA groups.

3.4. Effect of TAU on anti- and pro-apoptosis markers in NMDA-exposed retina

3.4.1. TUNEL

The number of TUNEL positive cells in the GCL was highest in the NMDA group, amounting to 3.85- fold higher number than that in the PBS group ($p < 0.001$). TAU pre-treatment significantly decreased NMDA-induced retinal cell apoptosis, with a 40% difference from NMDA group ($p < 0.05$). However, TUNEL positive cell count remained 2.32- fold higher in TAU pre-treatment group compared to PBS group ($p < 0.05$). There were no significant differences between the co- or post-treated TAU groups and those of the NMDA group (Fig. 6).

3.4.2. Active caspase-3 immunohistochemistry

On average, the most abundant caspase-3 staining was observed in the NMDA group, compared to PBS and TAU treated groups. These results correspond to TUNEL staining results. Quantitative measurement showed that in the NMDA group number of caspase positive cells was significantly higher than in the PBS group, by 5.5- fold ($p < 0.001$; Fig. 7). The caspase-3 staining was significantly lower in the pre- and co-treated TAU groups compared to NMDA group, by 55% ($p < 0.001$) and 38% ($p < 0.01$), respectively. Additionally, in both the co- and post-treated TAU groups, a greater number of caspase-3 positive cells were observed than in the pre-treatment group, by 1.36- and 1.75- fold, respectively.

3.4.3. Bcl-2

Down-regulation of the Bcl-2 protein is associated with apoptosis. The most prominent down-regulation of the Bcl-2 level was observed in

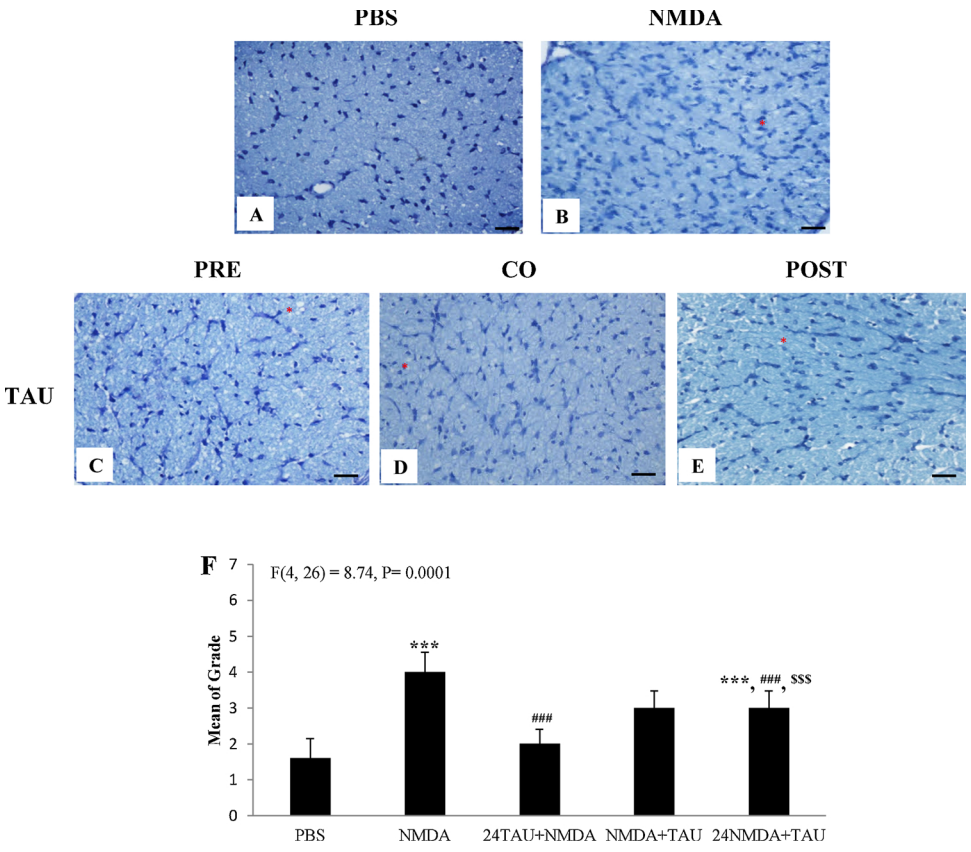

Fig. 4. Representative light micrographs of toluidine blue–stained optic nerve (ON) semithin sections (40X). Groups **A** (PBS) control, **B** (NMDA), **C (**24TAU + NMDA) pretreatment, **D** (NMDA + TAU) co-treatment, **E** (24NMDA + TAU) post-treatment. **F** The mean of grade. **A** Normal cross section of intact optic nerve in control group. **B** Extensive glial cells distribution occupying the entire section. **C** Comparable distribution of glial cells to the control group with slight degeneration of nerve fibers. **D** Denser glial cells. **E** Presence of glial cells and vacuolation indicates progressive degenerative changes. Data expressed as the mean and SD. Statistical significances were analyzed using one-way ANOVA with Bonferroni correction test: $^{***}p < 0.001$ versus PBS group, $^{\#\#\#}p < 0.001$ versus NMDA group and $^{\$\$\$}p < 0.01$ versus 24TAU + NMDA group. * Indicates degenerating nerve fibers. (Scale bar 50 μm).

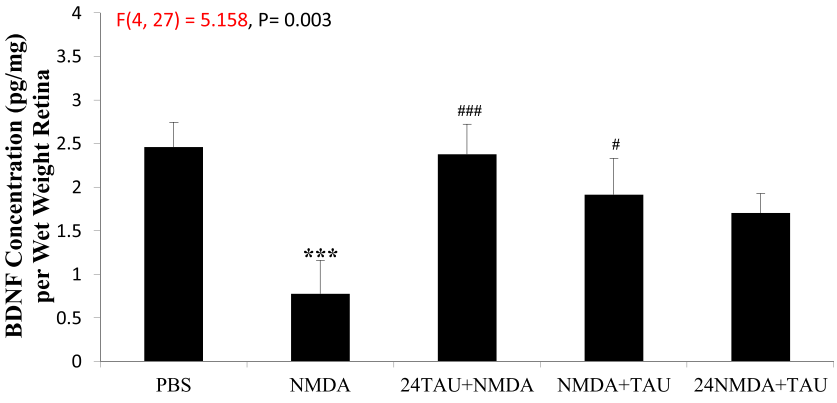

Fig. 5. Quantification of protein levels of BDNF in the rat retina 7 days after the treatment. BDNF protein levels were determined by ELISA and are shown as the quantity of neurotrophin per retina (in picograms/milligram). Groups (PBS) control, (NMDA), **(**24TAU + NMDA) pretreatment, (NMDA + TAU) co-treatment, (24NMDA + TAU) post-treatment. Data expressed as the mean and SD. Statistical significances were analyzed using one way ANOVA with Bonferroni correction test: $^{***}p < 0.01$ versus PBS group, $^{\#}p < 0.05$ versus NMDA group, $^{\#\#\#}p < 0.001$ versus NMDA group.

the NMDA group. As shown in Fig. 8A, the NMDA group exhibited a significantly lower level of Bcl-2 protein than the PBS group, by 65% ($p < 0.001$). All TAU treated groups showed significantly increased Bcl-2 levels, compared to the levels observed in the NMDA group, by 2.80- ($p < 0.001$), 2.82- ($p < 0.001$) and 2.24- fold ($p < 0.001$), in pre-, co- and post-treatment groups, respectively.

3.4.4. Bax (Bcl-2 associated X protein)

In contrast to the Bcl-2 protein level, the expression of the pro-apoptotic Bax protein showed the highest expression in the NMDA group (Fig. 8B). The mean Bax level in the NMDA group was significantly higher than that in the PBS group, by 1.71-fold ($p < 0.001$). TAU pre-treated group showed significantly lower expression of Bax compared to NMDA group (34%; $p < 0.01$) indicating protective effect of TAU. However, no significant differences were observed in the Bax level between the NMDA group and co- or post-treatment TAU groups.

3.4.5. Active caspase-3 assay

In agreement with the Bax and Bcl-2 protein expressions, retinal caspase-3 expression in the NMDA group was significantly higher than in the PBS group, at 3.54- folds ($p < 0.001$; Fig. 9). A clear protective effect of TAU against NMDA excitotoxicity was exhibited in the group that was pre-treated with TAU, as indicated by a significant reduction in the level of caspase-3 staining compared to the NMDA group, by 36%($p < 0.001$). Caspase-3 staining in both groups that were co- and post-treated with TAU was comparable to that in the NMDA group, despite lower caspase 3 activity.

4. Discussion

The progressive loss of RGCs, resulting in visual deficit, is a hallmark of glaucoma (Sucher et al., 1997; Guerin et al., 2006; Agarwal et al., 2009). Glutamate excitotoxicity has been implicated in the pathogenesis of a number of chronic neurodegenerative diseases,

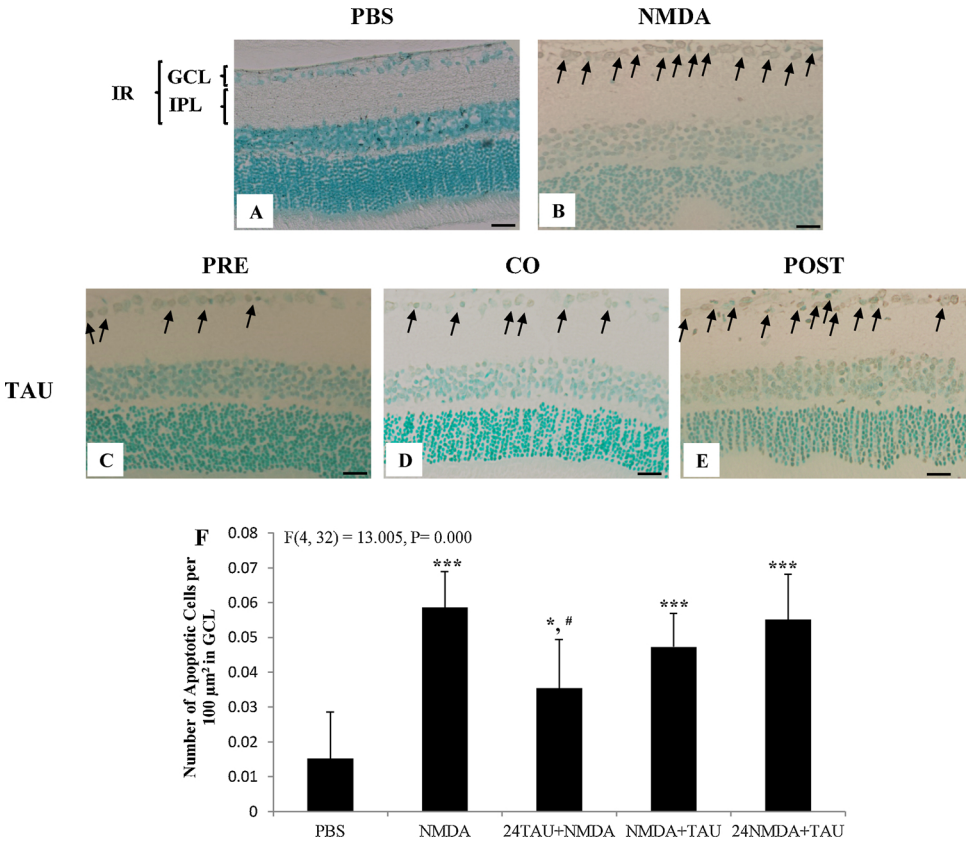

Fig. 6. Representative microphotographs of retinal sections from each of the groups stained in TUNEL-IHC staining at 20× magnification. Arrow indicates TUNEL-positive cells. Groups **A** (PBS) control, **B** (NMDA), **C** (24TAU + NMDA) pretreatment, **D** (NMDA + TAU) co-treatment, **E** (24NMDA + TAU) post-treatment. **A** No apoptotic signal was detected in the GCL. **B** Numerous detection of apoptosis ganglion cells. **C** Exhibits only a few of apoptotic ganglion cells. **D** Several apoptotic signals were detected. **E** A multiple presence of apoptotic ganglion cells was observed. **F** Number of apoptotic cells per 100 µm^2 in GCL. Data expressed as the mean and SD. Statistical significances were analyzed using one-way ANOVA with Bonferroni correction test: *p < 0.05 versus PBS group, ***p < 0.001 versus PBS group and $^{\#}$p < 0.05 versus NMDA group. GCL= ganglion cell layer, IPL= inner plexiform layer, IR= inner retina. (Scale bar = 100 µm).

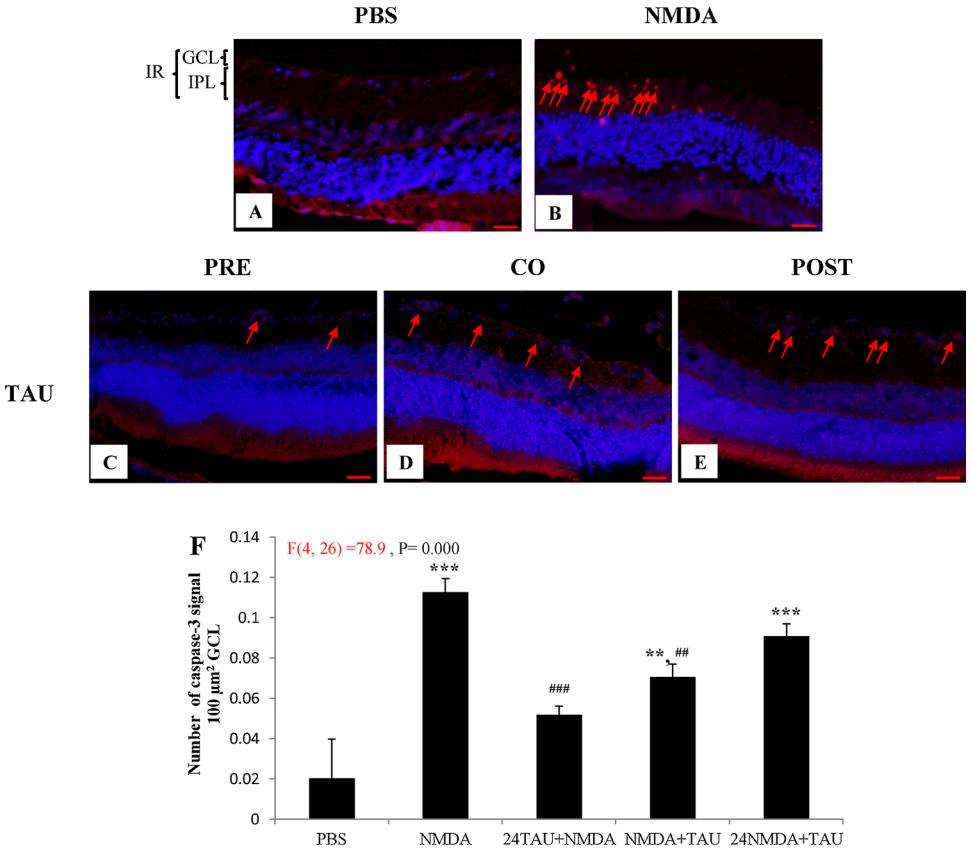

Fig. 7. Representative microphotographs of retinal sections from each of the groups stained (red) with Caspase-3 immunofluorescence and DAPI (blue) at 60X magnification. Arrow (red) indicates caspase-3 positive cells. Groups **A** (PBS) control, **B** (NMDA), **C** (24TAU + NMD) pretreatment, **D** (NMDA + TAU) co-treatment, **E** (24NMDA + TAU) post-treatment. The most abundant caspase positive cells were detected in NMDA group. Only few caspase positive cells were detected in TAU treatment groups particularly in pretreatment group. **F** Number of caspase-3 positive cells per 100 µm^2 of GCL. Data expressed as the mean and SD. Statistical significances were analyzed using one-way ANOVA with Bonferroni correction test: **p < 0.01 versus PBS group, ***p < 0.001 versus PBS group, $^{\#\#}$p < 0.01 versus NMDA group, $^{\#\#\#}$p < 0.001 versus NMDA group. GCL= ganglion cell layer, IPL= inner plexiform layer, IR= inner retina. (Scale bar 100 µm).

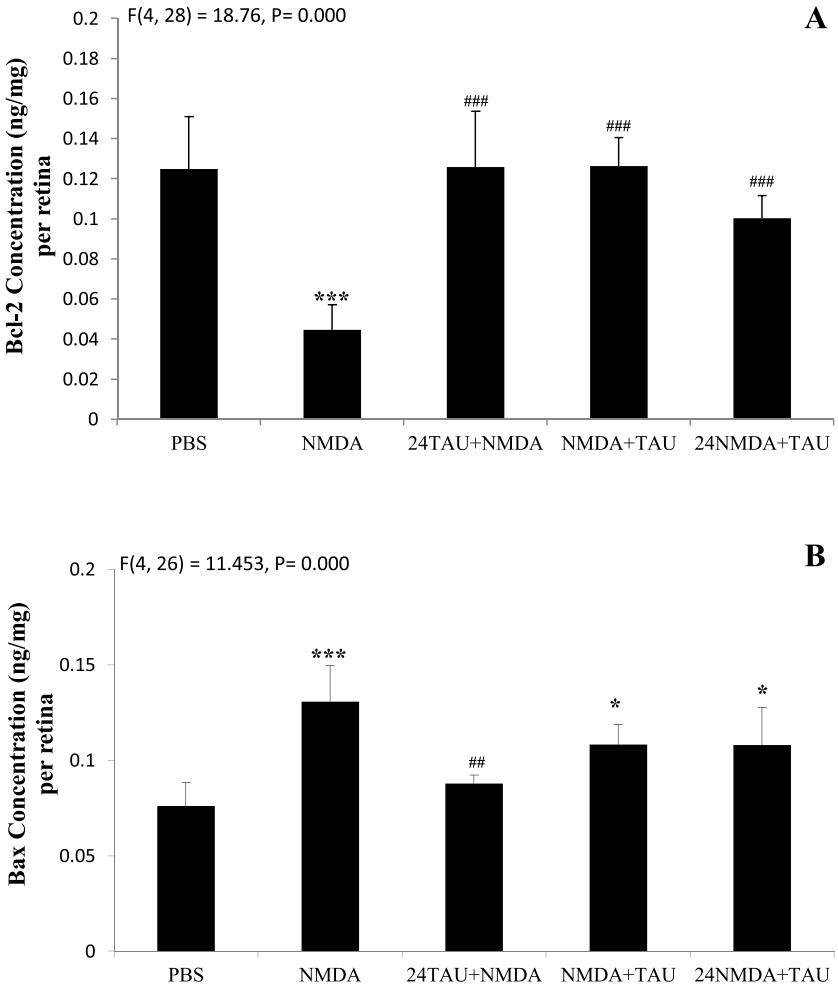

Fig. 8. Quantification of protein levels of (**A**) Bcl-2 and (**B**) Bax in the rat retina 7 days after the treatment. The protein levels were determined by ELISA and are shown as the quantity per retina (in nanograms/milligram). Groups (PBS) control, (NMDA), (24TAU + NMDA) pretreatment, (NMDA + TAU) co-treatment, (24NMDA + TAU) post-treatment. Data expressed as the mean and SD. Statistical significances were analyzed using one-way ANOVA with Bonferroni correction test: *p < 0.05 versus PBS group, ***p < 0.001 versus PBS group, $^{\#\#}$p < 0.01 versus NMDA, and $^{\#\#\#}$p < 0.001 versus NMDA group.

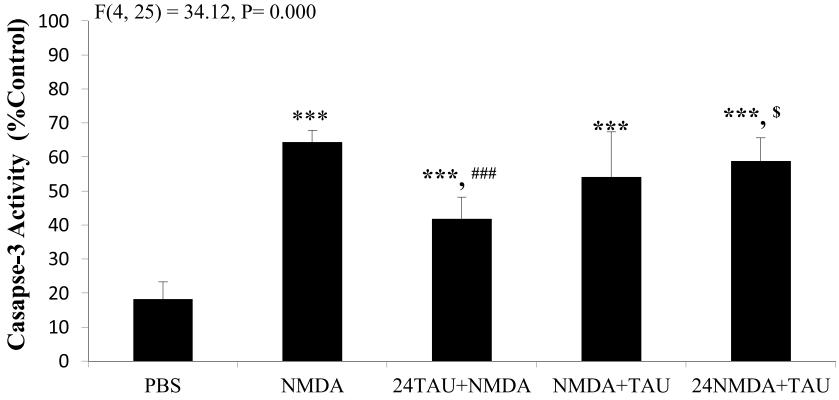

Fig. 9. Retinal activity of caspase-3 following NMDA induced and TAU treatment. Data are given as mean of percentage Casapase-3 positive from OD units S.E.M. per min and weight of retina as a measurement of DEVD-AMC cleavage by active caspase-3. Groups (PBS) control, (NMDA), (24TAU + NMDA) pretreatment, (NMDA + TAU) co-treatment, (24NMDA + TAU) post-treatment. Statistical significances were analyzed using one-way ANOVA with Bonferroni correction test: ***p < 0.001 versus PBS group, $^{\#\#\#}$p < 0.001 versus NMDA group and $^{\$}$p < 0.05 versus 24TAU + NMDA group.

including glaucoma (Vorwerk et al., 1999; Kuehn et al., 2005; Seki & Lipton, 2008).

TAU is a free amino sulfonic acid that is particularly abundant in the retina. It demonstrates multiple cellular functions, including a central role as a neurotransmitter as well as a trophic factor in CNS development, as an osmolyte, as a neuromodulator, and as a neuroprotectant. It also plays a role in the maintenance of the structural integrity of the membrane and in the regulation of calcium transport and homeostasis. The neurotransmitter properties of TAU are illustrated by its ability to elicit neuronal hyperpolarisation, by the presence of specific TAU synthesising enzymes and receptors in the CNS, and by the presence of a TAU transporter system (Schacknow & Samples, 2010). TAU has been widely documented to be a neuroprotective agent against a variety of insults in which glutamate excitotoxicity is implicated. In the present study, we investigated the anti-apoptotic effects of TAU against NMDA-induced retinal excitotoxicity in rats.

The loss of retinal neurons in the GCL is a hallmark of glaucoma. In our study, analysis of apoptotic cells, using the TUNEL assay, revealed

that the number of TUNEL-positive (apoptotic) cells was significantly higher in the GCL on day 7 of NMDA exposure. Similarly, the number of apoptotic cells was significantly lower in the retinae of rats treated with TAU. Consistent with an alteration in cell apoptosis, H&E-stained retinal sections showed that the number of neuronal cells in the GCL was strikingly lower in the retina 7 days after NMDA exposure than in the untreated retina. By contrast, retinal cells were preserved in retinae of animals that were treated with TAU.

The final common pathway for any neuronal injury is necrosis or apoptosis, the latter of which plays a major role in RGC death in glaucoma. Regardless of the initiating injury, there is an activation of the caspase cascade (Green, 1998), increased expression of pro-apoptotic genes, such as Bax/Bid (Oltvai & Korsmeyer, 1994), and down-regulation of anti-apoptotic genes, such as Bcl-2/Bcl-xl (Levin et al., 1997), leading to non-inflammatory programmed cell death (Quigley, 1999). NMDA exposure increases the ratio of the pro-apoptotic protein Bax to the anti-apoptotic protein Bcl-2 by directly cleaving Bax to an activated form through a mitochondrial pathway (Wood & Newcomb, 2000). Activated Bax forms multimers in the mitochondria, with subsequent cytochrome c release, which ultimately contributes to apoptosis through the formation of the apoptosome protein complex and activation of downstream caspases 3 and 7 (Li et al., 1997).

TAU exerts its neuroprotective functions against glutamate induced excitotoxicity by reducing the glutamate-induced increase in the intracellular calcium level (Yu et al., 2008; Leon et al., 2009; Froger et al., 2012; Ye et al., 2013). It is generally believed that the neuroprotective functions of TAU are due to its role in the reduction of the intracellular free Ca^{2+} concentration, $[Ca^{2+}]$, and its anti-oxidative stress capacity (Chen et al., 2001; Schaffer et al., 2003). The results of our study are in line with those of the study of Leon and colleagues (Leon et al., 2009), which showed that TAU can shift the ratio of the anti-apoptotic protein, Bcl-2 and the pro-apoptotic protein, Bax, in favour of cell survival (Leon et al., 2009). In addition, the same authors have also demonstrated that glutamate-induced activation of calpain is inhibited by TAU, resulting in a decrease in the formation of TAU hetero-dimers of Bcl-2 and Bax, and the subsequent release of cytochrome C and the apoptosis cascade (Leon et al., 2009).

BDNF, a member of the neurotrophin family of growth factors, plays a pivotal role in the maintenance of normal neuronal development. Several reports have shown that neurotrophic agents, particularly BDNF in RGCs, are implicated in the maintenance and promotion of development activities in the CNS through *in vivo* experiments (Vecino et al., 1999; Quigley et al., 2000; Urcola & Vecino, 2008). Neurotrophin deprivation has been proposed as one of the mechanisms involved in apoptosis of RGCs in glaucoma, whereby retrograde axonal transport is blocked through IOP elevation (Quigley & Addicks, 1980). It has been suggested that inhibition of the transport of BDNF to the retina from the superior colliculus might be the underlying mechanism of RGC death in glaucoma. In experimental animal models of glaucoma, BDNF transport to the retina was found to be severely reduced (Pease et al., 2000; Quigley et al., 2000). In this study, the BDNF level was substantially lower in the NMDA exposed retinae, while administration of TAU promoted cell survival through enhanced expression of BDNF. However, NMDA neurotoxicity alone has been reported to be involved in the increase in the BDNF level (Vecino et al., 1999).

5. Conclusion

In conclusion, current study revealed that pre-treatment with intravitreal TAU prevents the NMDA-induced apoptosis of retinal cells in inner retina. Overall, our data demonstrate that pre-treatment with TAU was more effective against NMDA-induced retinal cell apoptosis compared to co- or post-treatment with TAU indicating more of a protective effect. This protective effect of TAU seems to be associated with activation of BDNF-related neuroprotective mechanisms.

Declaration of interest

The authors acknowledge the financial support provided by the Institute of Research Management & Innovation (IRMI), Universiti Teknologi MARA, Malaysia, under the grant no. 600-IRMI/MYRA 5/3/BESTARI (004/2017).

Competing interests

The authors declare that there are no competing interests.

Transparency document

The Transparency document associated with this article can be found in the online version.

Acknowledgement

We acknowledge the administrative and facility support provided by the Research Management Institute, the Institute of Medical Molecular Biotechnology (IMMB) and the Laboratory Animal Care Unit at Universiti Teknologi MARA, Malaysia

References

Agarwal, R., Gupta, S.K., Agarwal, P., Saxena, R., Agrawal, S.S., 2009. Current concepts in the pathophysiology of glaucoma. Indian J. Ophthalmol. 57 (4), 257–266. https://doi.org/10.4103/0301-4738.53049.

Arfuzir, N.N., Lambuk, L., Jafri, A.J., Agarwal, R., Iezhitsa, I., Sidek, S., Agarwal, P., Bakar, N.S., Kutty, M.K., Yusof, A.P., Krasilnikova, A., Spasov, A., Ozerov, A., Mohd Ismail, N., 2016. Protective effect of magnesium acetyltaurate against endothelin-induced retinal and optic nerve injury. Neurosci 325, 153–164. https://doi.org/10.1016/j.neuroscience.

Arfuzir, N.N., Agarwal, R., Iezhitsa, I., Agarwal, P., Sidek, S., Ismail, N.M., 2018. Taurine protects against retinal and optic nerve damage induced by endothelin-1 in rats via antioxidant effects. Neural Regen. Res. 13 (11), 2014–2021. https://doi.org/10.4103/1673-5374.239450.

Baltmr, A., Duggan, J., Nizari, S., Salt, T.E., Cordeiro, M.F., 2010. Neuroprotection in glaucoma – is there a future role? Exp. Eye. Res. 91 (5), 554–566. https://doi.org/10.1016/j.exer.2010.08.009.

Casson, R.J., Franzco, D., Chidlow, G., Wood, J.P.M., Crowston, J.G., Franzco, I.G., 2012. Review Definition of glaucoma: clinical and experimental concepts. Clin. Experiment. Ophthalmol. 341–349. https://doi.org/10.1111/j.1442-9071.2012.02773.x.

Chen, W.Q., Nguyen, M., Carr, J., Lee, Y.J., Jin, H., Foos, T., Hsu, C.C., Davis, K.M., Schloss, J.V., Wu, J.Y., 2001. Role of taurine in regulation of intracellular calcium level and neuroprotective function in cultured neurons. J. Neurosci. Res. 66, 612–619. https://doi.org/10.1002/jnr.10027.

Chen, F., Jiang, L., Shen, C., Wan, H., Xu, L., Wang, N., Jonas, J.B., 2012. Neuroprotective effect of against N -methyl-d-aspartate- induced excitotoxicity in the adult rat retina. Acta Opthalmol. 609–615. https://doi.org/10.1111/j.1755-3768.2012.02502.x.

Ebneter, A., Casson, R.J., Wood, J.P.M., Chidlow, G., 2010. Microglial Activation in the Visual Pathway in Experimental Glaucoma: Spatiotemporal Characterization and Correlation with Axonal Injury. Invest. Ophthalmol. Vis. Sci. 6448–6460. https://doi.org/10.1167/iovs.10-5284.

Ebneter, A., Chidlow, G., Wood, J.P.M., Casson, R.J., 2011. Protection of retinal ganglion cells and the optic nerve during short-term hyperglycemia in experimental glaucoma. Arch. Ophthalmol. 129 (10), 1337–1344. https://doi.org/10.1001/archophthalmol.2011.269.

El Idrissi, A., 2008. Taurine increases mitochondrial buffering of calcium: role in neuroprotection. Amino acids 34 (2), 321–328. https://doi.org/10.1007/s00726-006-0396-9.

Froger, N., Cadetti, L., Lorach, H., Martins, J., Bemelmans, A.P., Dubus, E., Picaud, S., 2012. Taurine Provides Neuroprotection against Retinal Ganglion Cell Degeneration. PLoS ONE 7 (10). https://doi.org/10.1371/journal.pone.0042017.

Froger, N., Moutsimilli, L., Cadetti, L., Jammoul, F., Wang, Q.P., Fan, Y., Sahel, J.A., 2014. Taurine: the comeback of a neutraceutical in the prevention of retinal degenerations. Prog. Retin. Eye Res. 41, 44–63.

Goldblum, D., Mittag, T., 2002. Prospects for relevant glaucoma models with retinal ganglion cell damage in the rodent eye. Vision Res. 42 (4), 471–478. https://doi.org/10.1016/S0042-6989(01)00194-8.

Green, D.R., 1998. Apoptotic pathways: the roads to ruin. Cell 94 (6), 695–698.

Guerin, M.B., McKernan, D.P., O'Brien, C.J., Cotter, T.G., 2006. Retinal ganglion cells: Dying to survive. Int. J. Dev. Biol. 50 (8), 665–674. https://doi.org/10.1387/ijdb.062159mg.

Hayes, K.C., Carey, R.E., Schmidt, S.Y., 1975. Retinal degeneration associated with taurine deficiency in the cat. Science 188 (4191), 949–951.

Iezhitsa, I., Agarwal, R., 2018. Magnesium acethyltaurate as a potential agent for retinal and optic nerve protection in glaucoma. Neural. Regen. Res. 13 (5), 807–808.

https://doi.org/10.4103/1673-5374.232470.
Imaki, H., Moretz, R., Wisniewski, H., Neuringer, M., Sturman, J., 1987. Retinal degeneration in 3-month-old rhesus monkey infants fed a taurine-free human infant formula. J. Neurosc. Res. 18 (4), 602–614.
Jafri, A.J.A., Arfuzir, N.N.N., Lambuk, L., Iezhitsa, I., Agarwal, R., Agarwal, P., Razali, N., Krasilnikova, A., Kharitonova, M., Demidov, V., Serebryansky, E., Skalny, A., Spasov, A., Yusof, A.P.M., Ismail, N.M., 2017. Protective effect of magnesium acetyltaurate against NMDA-induced retinal damage involves restoration of minerals and trace elements homeostasis. J. Trace Elem. Med. Biol. 39, 147–154. https://doi.org/10.1016/j.jtemb.2016.09.005.
Jafri, A.J., Agarwal, R., Iezhitsa, I., Agarwal, P., Spasov, A., Ozerov, A., Ismail, N.M., 2018. Protective effect of magnesium acetyltaurate and taurine against NMDA-induced retinal damage involves reduced nitrosative stress. Mol. Vis. 24, 495–508.
Jia, L., Cepurna, W.O., Johnson, E.C., Morrison, J.C., 2000. Patterns of intraocular pressure elevation after aqueous humor outflow obstruction in rats. Invest. Ophthalmol. Vis. Sci. 41 (6), 1380–1385.
Joo, C.K., Choi, J.S., Ko, H.W., Park, K.Y., Sohn, S., Chun, M.H., Gwag, B.J., 1999. Necrosis and apoptosis after retinal ischemia: Involvement of NMDA- mediated excitotoxicity and p53. Invest. Ophthalmol. Vis. Sci. 40 (3), 713–720.
Khatib, T.Z., Martin, K.R., 2017. Protecting retinal ganglion cells. Eye 31 (2), 218–224. https://doi.org/10.1038/eye.2016.299. Epub 2017 Jan 13.
Kuehn, M.H., Fingert, J.H., Kwon, Y.H., 2005. Retinal Ganglion Cell Death in Glaucoma: Mechanisms and Neuroprotective Strategies. Opthalmol. Clin. N. Am. 18, 383–395. https://doi.org/10.1016/j.ohc.2005.04.002.
Labes, M., Thomsen, S., Srinivasan, A., Ba, M., 1999. Activation of caspase-3 in axotomized rat retinal ganglion cells in vivo. FEBS Lett. 453, 361–364.
Lambert, I.H., Kristensen, D.M., Holm, J.B., Mortensen, O.H., 2015. Physiological role of taurine–from organism to organelle. Acta Physiol. (Oxf.) 213 (1), 191–212. https://doi.org/10.1111/apha.12365.
Lambuk, L., Jafri, A.J., Arfuzir, N.N., Iezhitsa, I., Agarwal, R., Rozali, K.N., Agarwal, P., Bakar, N.S., Kutty, M.K., Yusof, A.P., Krasilnikova, A., Spasov, A., Ozerov, A., Ismail, N.M., 2017. Neuroprotective Effect of Magnesium Acetyltaurate Against NMDA-Induced Excitotoxicity in Rat Retina. Neurotox. Res. 31 (1), 31–45. https://doi.org/10.1007/s12640-016-9658-9.
Leon, R., Wu, H., Jin, Y., Wei, J., Buddhala, C., Prentice, H., Wu, J.Y., 2009. Protective function of taurine in glutamate-induced apoptosis in cultured neurons. J. Neurosci. Res. 87 (5), 1185–1194. https://doi.org/10.1002/jnr.21926.
Levin, L.A., Schlamp, C.L., Spieldoch, R.L., Geszvain, K.M., Nickells, R.W., 1997. Identification of the Bcl-2 family of genes in the rat retina. Invest. Ophthalmol. Vis. Sci. 38 (12), 2545–2553.
Li, P., Nijhawan, D., Budihardjo, I., 1997. Cytochrome c and dATP-dependent formation of Apaf-1/caspase-9 complex initiates an apoptotic protease cascade. Cell 91, 479–489.
Macaione, S., Ruggeri, P., Luca, F.D., Tucci, G., 1974. Free amino acids in developing rat retina. J. Neurochem. 22 (6), 887–891.
Militante, J.D., Lombardini, J.B., 2002. Taurine: Evidence of physiological function in the retina. Nutr. Neurosci. 5 (2), 75–90. https://doi.org/10.1080/10284150290018991.
Mozaffarieh, M., Flammer, J., 2007. Is There More to Glaucoma Treatment Than Lowering IOP? J. Surv. Opthal. 52, 174–179. https://doi.org/10.1016/j.survophthal.2007.08.013.
Mozaffarieh, M., Flammer, J., 2013. New insights in the pathogenesis and treatment of normal tension glaucoma. Curr. Opin. Pharmacol. 13 (1), 43–49.
Naskar, R., Vorwerk, C.K., Dreyer, E.B., 2000. Concurrent Downregulation of a Glutamate Transporter and Receptor in Glaucoma. Invest. Ophthalmol. Vis. Sci. 41 (7), 1940–1944.
Nor Arfuzir, N.N., Agarwal, R., Iezhitsa, I., Agarwal, P., Sidek, S., Spasov, A., Ozerov, A., Mohd Ismail, N., 2018. Effect of magnesium acetyltaurate and taurine on endothelin1-induced retinal nitrosative stress in rats. Curr. Eye. Res 1–9. https://doi.org/10.1080/02713683.2018.1467933.
Ohzeki, T., Machida, S., Takahashi, T., Ohtaka, K., 2007. The Effect of Intravitreal N -Methyl- DL -Aspartic Acid on the Electroretinogram in Royal College of Surgeons Rats. Acta. Anat. 165–174. https://doi.org/10.1007/s10384-007-0420-y.
Oltvai, Z.N., Korsmeyer, S.J., 1994. Checkpoints of dueling dimers foil death wishes. Cell 79 (2), 189–192.
Pease, M.E., McKinnon, S.J., Quigley, H.A., Kerrigan-Baumrind, L.A., Zack, D.J., 2000. Obstructed axonal transport of BDNF and its receptor TrkB in experimental glaucoma. Invest. Ophthalmol. Vis. Sci. 41 (3), 764–774.
Quigley, H.A., 1999. Neuronal death in glaucoma. Prog. Retin. Eye Res. 18 (1), 39–57.
Quigley, H.A., Broman, A.T., 2006. The number of people with glaucoma worldwide in 2010 and 2020. Community Eye Health J. 19 (59), 35.
Quigley, H., 2018. The Number of People with Glaucoma Worldwide in 2010 and 2020. Br. J. Opthalmol. 90, 262–268. https://doi.org/10.1136/bjo.2005.081224.
Quigley, H.A., Addicks, E.M., 1980. Chronic experimental glaucoma in primates. Invest. Ophthalmol. Vis. Sci. 126–136.
Quigley, H.A., McKinnon, S.J., Zack, D.J., Pease, M.E., Kerrigan-Baumrind, L.A., Kerrigan, D.F., Mitchell, R.S., 2000. Retrograde axonal transport of BDNF in retinal ganglion cells is blocked by acute IOP elevation in rats. Invest. Ophthalmol. Vis. Sci 41 (11), 3460–3466.
Razali, N., Agarwal, R., Agarwal, P., 2014. Anterior and posterior segment changes in rat eyes with chronic steroid administration and their responsiveness to antiglaucoma drugs. Eur. J. Pharmacol. 1–8. https://doi.org/10.1016/j.ejphar.2014.11.029.
Schacknow, P.N., Samples, J.R. (Eds.), 2010. The Glaucoma Book: A Practical, Evidence-Based Approach to Patient Care. Springer Science + Business Media, LLC. https://doi.org/10.1007/978-0-387-76700-0_56.
Schaffer, S., Azuma, J., Takahashi, K., Mozaffari, M., 2003. Why Is Taurine Cytoprotective? In: In: Lombardini, J.B., Schaffer, S.W., Azuma, J. (Eds.), Taurine 5. Advances in Experimental Medicine and Biology 526 Springer, Boston, MA. https://doi.org/10.1007/978-1-4615-0077-3_39.
Seki, M., Lipton, S.A., 2008. Targeting excitotoxic/free radical signaling pathways for therapeutic intervention in glaucoma. Prog. Brain Res. 173 (8), 495–510. https://doi.org/10.1016/S0079-6123(08)01134-5.
Sucher, N.J., Lipton, S.A., Dreyer, E.B., 1997. Molecular Basis of Glutamate Toxicity in Retinal Ganglion Cells. Vision. Res. 37 (24), 3483–3493. https://doi.org/10.1016/S0042-6989(97)00047-3.
Takahata, K., Katsuki, H., Kume, T., Nakata, D., Ito, K., Muraoka, S., Akaike, A., 2003. Retinal neuronal death induced by intraocular administration of a nitric oxide donor and its rescue by neurotrophic factors in rats. Invest. Ophthalmol. Vis. Sci. 44 (4), 1760–1766. https://doi.org/10.1167/iovs.02-0471.
Tham, Y.C., Li, X., Wong, T.Y., Quigley, H.A., Aung, T., Cheng, C.Y., 2014. Global prevalence of glaucoma and projections of glaucoma burden through 2040: a systematic review and meta-analysis. Ophthalmol 121 (11), 2081–2090. https://doi.org/10.1016/j.ophtha.2014.05.013.
Urcola, J.H., Vecino, E., 2008. Retinal ganglion cell neuroprotection in a rat model of glaucoma following brimonidine, latanoprost or combined treatments. Exp. Eye Res. 86, 798–806. https://doi.org/10.1016/j.exer.2008.02.008.
Vasudevan, S.K., Gupta, V., Crowston, J.G., 2011. Neuroprotection in glaucoma. Indian J. Ophthalmol. 59 (Suppl), S102–S113. https://doi.org/10.4103/0301-4738.73700.
Vecino, E., Ugarte, M., Nash, M.S., Osborne, N.N., 1999. NMDA induces BDNF expression in the albino rat retina in vivo. Neuroreport 10 (5), 1103–1106.
Vorwerk, C.K., Gorla, M.S.R., Dreyer, E.B., 1999. An experimental basis for implicating excitotoxicity in glaucomatous optic neuropathy. Surv. Ophthalmol. 43 (6 SUPPL). https://doi.org/10.1016/S0039-6257(99)00017-X.
Wood, D.E., Newcomb, E.W., 2000. Cleavage of Bax enhances its cell death function. Exp. Cell Res. 256, 375–382. https://doi.org/10.1006/excr.2000.4859.
Wu, J.Y., Prentice, H., 2010. Role of taurine in the central nervous system. J. Biomed. Sci. 17 (1). https://doi.org/10.1186/1423-0127-17-S1-S1.
Ye, H.B., Shi, H.B., Yin, S.K., 2013. Mechanisms underlying taurine protection against glutamate-induced neurotoxicity. Can. J. Neurol. Sci. 40 (5), 628–634. https://doi.org/10.1017/S0317167100014840.
Yu, X., Xu, Z., Mi, M., Xu, H., Zhu, J., Wei, N., Tang, Y., 2008. Dietary taurine supplementation ameliorates diabetic retinopathy via anti-excitotoxicity of glutamate in streptozotocin-induced sprague-dawley rats. Neurochem. Res. 33 (3), 500–507. https://doi.org/10.1007/s11064-007-9465-z.